UNIVERSITÀ DI PARMA
ARCHIVIO DELLA RICERCA

University of Parma Research Repository

Binding and Reactivity of Copper to R1 and R3 Fragments of tau Protein

note finali coverpage

(Article begins on next page)

22 December 2024

Binding and reactivity of copper to R1 and R3 fragments of tau protein

Chiara Bacchella,[a] Silvia Gentili,[b] Denise Bellotti,[c] Eleonora Quartieri,[b] Sara Draghi,[d] Maria Camilla Baratto,[d] Maurizio Remelli,[c] Daniela Valensin,[d] Enrico Monzani,[a] Stefania Nicolis,[a] Luigi Casella,[a] Matteo Tegoni,*[b] Simone Dell'Acqua*[a]

[a.] Dipartimento di Chimica, Università di Pavia, Via Taramelli 12, 27100 Pavia, Italy

[b.] Dipartimento di Scienze Chimiche, della Vita e della Sostenibilità Ambientale, Università di Parma, Parco Area delle Scienze 11/A, 43124 Parma, Italy

[c.] Dipartimento di Scienze Chimiche e Farmaceutiche, Università di Ferrara, Via Luigi Borsari 46, 44121 Ferrara, Italy

[d.] Dipartimento di Biotecnologie, Chimica e Farmacia, Università di Siena, Via A. Moro 2, 53100, Siena, Italy

Tau protein • Copper complexes • Alzheimer's disease • Oxidative stress • Post-translational protein modification

ABSTRACT: Tau protein is present in significant amounts in neurons, where it contributes to the stabilization of microtubules. Insoluble neurofibrillary tangles of tau are associated with several neurological disorders known as tauopathies, among which is Alzheimer's disease. In neurons, tau binds tubulin through its microtubule binding domain which comprises four imperfect repeats (R1-R4). The histidine residues contained in these fragments are potential binding sites for metal ions and are located close to the regions that drive the formation of amyloid aggregates of tau. In this study, we present a detailed characterization through potentiometric and spectroscopic methods of the binding of copper in both oxidation states to R1 and R3 peptides, which contain one and two histidine residues, respectively. We also evaluate how the redox cycling of copper bound to tau peptides can mediate oxidation that can potentially target exogenous substrates such as neuronal catecholamines. The resulting quinone oxidation products undergo oligomerization and can competitively give post-translational peptide modifications yielding catechol adducts at amino acid residues. The presence of His-His tandem in R3 peptide strongly influences both the binding of copper and the reactivity of the resulting copper complex. In particular, the presence of the two adjacent histidines makes the copper(I) binding to R3 much stronger than in R1. The copper-R3 complex is also much more active than copper-R1 complex in promoting oxidative reactions, indicating that the two neighbouring histidines activate copper as a catalyst in molecular oxygen activation reactions.

INTRODUCTION

Tau proteins, firstly discovered and characterized in 1975,[1] are present in the axon terminals of neurons and are mostly associated with microtubules, the major constituent of the cytoskeleton, composed of a dynamic tubulin polymer. In solution, tau proteins are highly unfolded and characterized by high flexibility of the chain.[2] The human brain contains six main tau isoforms that can be categorized depending on whether they contain three or four pseudorepeats (R1-R4) in the C-terminal region that constitutes the microtubule-binding domain. Tau proteins are highly soluble and show little tendency to aggregation. However, tau aggregation is characteristic of several neurodegenerative diseases known as tauopathies.[3-5] Among them, Alzheimer's disease (AD) is one of the most relevant and is characterized by the accumulation of extracellular amyloid plaques and intraneuronal tau neurofibrillary tangles (NFT).[6] The mechanism that leads to accumulation of NFT is still poorly understood, but there are evidences that tau undergoes post-translational modifications associated to AD such as abnormal hyperphosphorylation[7, 8] and nitration.[9] The failure of therapeutic approaches based on amyloid hypothesis has led to an increasing interest to tau mediated AD etiology.[10] Moreover, the recent application of cryo-electron microscopy (cryo-EM) technique has allowed a fundamental step for deciphering how the structural conformation might correlate physiological and pathological aspects of tau protein.[11] In particular, the structure of the tau fibrils from a diseased brain obtained with cryo-EM shows the formation of cross-β/β-helix structure between residues 306–378, which is the portion of tau comprising R3 and R4 regions.[12]

As for other neurodegenerative diseases, oxidative stress and metal ions are recognized as important factors contributing to AD etiology.[13-17] Copper, zinc, and iron are essential metals for healthy organisms and brain function, but impairment of metal homeostasis is a crucial risk fac-

tor.[18] Despite the large amount of biophysical and structural studies regarding the interaction of transition metals with other proteins related to neurodegeneration, such as α-synuclein,[19, 20] prion protein[21] and β-amyloid (Aβ),[22-24] much less is known about the interaction of metals ions with tau. The region encompassing the R1-R4 repeats represents potential binding site for metals, since each repeat contains at least one histidine (His268, His299 and His362 in R1, R2 and R4, respectively); R3 contains two vicinal histidine residues (His329 and His330) (Figure 1).
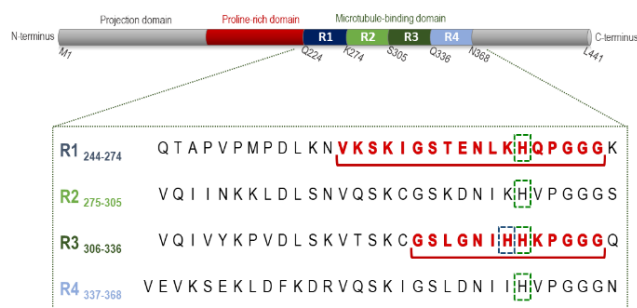

Figure 1 – Amino acid sequences of the four pseudorepeats in the longest tau isoform. Each pseudorepeat consists of 31-32 amino acid residues and contains a highly conserved octadecapeptide, which shows > 60 % homology. The fragments used in this study are underlined and highlighted in red and are defined as R1 (Ac-^{256}VKSKIGSTENLKHQPGGG^{273}-NH$_2$) and R3 (Ac-^{323}GSLGNIHHKPGGG^{335}-NH$_2$).

Isothermal titration calorimetry shows that zinc(II) binds to tau in a tetrahedral coordination site involving Cys291, Cys322 and two histidines with moderate micromolar affinity.[25] Moreover, zinc(II) promotes tau hyperphosphorylation by inactivation of protein phosphatase 2A.[26] Recently, an important role of zinc in the modulation of the aggregation process of R3-R4 has been proposed.[27]

Even if a detailed binding study is still missing, it has been suggested that iron(III) binds to hyperphosphorylated tau and induces its aggregation.[28] Regarding heme-iron, the analysis of the interaction with R1 fragment shows that heme binds with moderate affinity to the histidine contained in this region.[29]

The binding of copper to tau has been studied more extensively. In particular, Soragni et al. have suggested that copper(II) binds to a site between R2 and R3, even if a definite coordination sphere has not been proposed.[30] The binding of copper(II) to tau fragments R1,[31] R2[32] and R3[33] has been also reported showing the crucial role of histidine as coordination site; however, the peptide fragments used in these studies present free amine and carboxylic acid at the N-terminal and C-terminal respectively, giving rise to a coordination model which is not suitable for mimicking the binding to full length protein. The same objection can be made

with regards to an EPR spectroscopic study on the interaction of copper(II) and different portions of tau including R1, R2, R3 and R4 regions,[34] and a more recent study that analyses the interaction of copper, in both oxidation states, with R2 region.[35]

Another study suggests that also the N-terminal portion of tau protein can bind copper through coordination of His14 and His32.[36] The interaction of copper with the full length tau has been investigated also by laser ablation inductively coupled plasma mass spectrometry[37] and by electrochemical technique.[38] In particular, the latter study proposes a reduction potential for the Cu(II)/Cu(I) redox couple bound to tau protein of approximately 340 ± 5 mV versus NHE.

The number of studies that account for the reactivity of the copper-tau complexes and the related oxidative stress is even more limited. Sayre et al. analyzed the metal-catalyzed oxidation of 3,3'-diaminobenzidine in the presence of hydrogen peroxide and propose that copper and iron are involved in the redox reactions occurring in the neurofibrillary tangles as well as in the senile plaques.[39]

It is therefore crucial to better define the nature and strength of the binding of copper to tau by determining the stoichiometry and the structure of the complexes formed in solution and measuring the corresponding stability constants. In addition, the oxidative reactivity associated to these complexes should be explored to assess the potential contribution to oxidative stress arising from copper-tau interaction.

In the present study, we investigate the properties and the reactivity of the copper complexes formed with N-acetylated and C-amidated R1 (Ac-^{256}VKSKIGSTENLKHQPGGG^{273}-NH$_2$) and R3 (Ac-^{323}GSLGNIHHKPGGG^{335}-NH$_2$) fragments. These two fragments were chosen because they have different behavior in the NFT formation. In particular, R3 portion is found inside the cross-β/β-helix structure of tau filament whereas R1 is outside.[12] Moreover, these two peptides allow to clarify how the presence of one histidine or two vicinal histidines affects the affinity for copper and the reactivity of the relative copper-complexes. We also justify the choice to use a truncated R3 fragment excluding the cysteine residue (Cys322) according to the evidence that copper(II) is able to oxidize in vitro the cysteine residue inducing the formation of a disulfide intermolecular bond.[40] However, the two cysteine residues in tau protein (Cys291 and Cys322) are likely involved in disulfide bond in the native protein, even if formation of intramolecular or intermolecular bonds may play an important role in tau aggregation.[41, 42]

The speciation of the copper(I) and copper(II) complexes with both R1 and R3 peptides were studied by potentiometry, and the coordination environment of copper(II) in its adducts with the peptides was investigated by visible absorption and CD spectroscopy. The copper(I)- and copper(II)-R3 binding was also studied by NMR and EPR spectroscopy. Finally, we studied the oxidation of the dopamine (DA) neurotransmitter, as physiological model of induced copper redox cycling, and the related, but with a less

complex oxidation pattern, 4-methylcatechol (MC). The present study extends our previous investigations on the redox activity of copper complexes with neuronal peptide fragments of Aβ,[43-45] α-synuclein[46, 47] and prion protein.[48]

RESULTS AND DISCUSSION

Peptide protonation equilibria. R1 in its neutral form is a monoprotic acid (LH, Scheme S1). In its fully protonated form (on the side chains of Glu, His and the three Lys residues) it is a pentaprotic acid (LH_5^{4+}). The pK_a values determined by potentiometric titrations (Table 1) are fully consistent with the sequential deprotonation of the carboxylic group of Glu, the imidazolium nitrogen of His, and the three protonated amino groups of Lys residues, the latter ones occurring at pH > 8.5. At pH 7.4, the predominant form of R1 is LH_3^{2+}. The second peptide R3, in its neutral form has no acidic protons (L, Scheme S1) but it can undergo protonation on the imidazole rings of the two His residues and on the amino group of the Lys chain. In its fully protonated form it is therefore a triprotic acid (LH_3^{3+}). For this peptide the observed pK_a values (Table 1) are fully consistent with the deprotonation of the two His residues (in the pH range 4-8.5), and the deprotonation of the Lys side chain at pH > 9. At pH 7.4 the predominant form of R3 is LH^+.

Table 1. Protonation constants (pK_a) of the peptides R1 (LH) and R3 (L), and overall formation constants of their complexes with copper(II) (referred to the global reaction: $pCu + qL + rH = [Cu_pL_qH_r]$, charges omitted). $T = 298.2$ K, $I = 0.1$ M (KCl). Standard deviations on the last significant figure are given in parentheses. Most relevant species at neutral pH are given in bold.

	R1 = LH		R3 = L
pK_{a1}	4.16(3); COOH Glu	pK_{a1}	5.78(4) ($N_{im}H^+$ His)
pK_{a2}	6.40(2); $N_{im}H^+$ His	pK_{a2}	6.75(3) ($N_{im}H^+$ His)
pK_{a3}	9.69(1); NH_3^+ Lys	pK_{a3}	10.19(1) (NH_3^+ Lys)
pK_{a4}	10.32(1) NH_3^+ Lys		
pK_{a5}	10.64(1) NH_3^+ Lys		
Species	Log β	Species	Log β
$[Cu(LH_3)]^{4+}$	34.84(8)	-	-
$[Cu(LH_2)]^{3+}$	28.1(3)	$[Cu(LH_2)]^{4+}$	20.48(7)
$[Cu(LH)]^{2+}$	22.70(5)	$[Cu(LH)]^{3+}$	15.81(2)
$[CuL]^+$	14.08(8)	$[CuL]^{2+}$	9.39(3)
$[Cu(LH_{-1})]$	4.46(7)	$[Cu(LH_{-1})]^+$	2.48(2)
$[Cu(LH_{-2})]^-$	-5.85(9)	$[Cu(LH_{-2})]$	-6.22(3)
$[Cu(LH_{-3})]^{2-}$	-16.35(7)	$[Cu(LH_{-3})]^-$	-16.31(4)

Copper(II)/R1 complex formation equilibria. In the presence of copper(II), and in excess of ligand with respect equimolar metal:ligand ratio, the R1 peptide forms seven complex species. All these complexes correspond to 1:1 copper/peptide stoichiometry and differ for their protonation states. The stoichiometry of these species, along with their log β values, are reported in Table 1. A representative distribution diagram is reported in Figure 2. We will discuss here the speciation at neutral pH, whereas a complete description of the speciation of the systems is reported as Supporting Information. It should be highlighted that we did not examine in depth ligand:Cu ratios lower than 1.5 since reactivity experiments were principally carried out in the excess of peptide. Our conditions are therefore unfavourable for the formation of di- or polynuclear species that, in agreement with this perspective, were not found in our speciation systems.

The predominant species in the pH range 6 - 8.5 is $[Cu(LH)]^{2+}$ which reaches 95 % total copper at pH 7.2 (Figure 2). Above pH 8.5 $[CuL]^+$ becomes the most abundant species, reaching its maximum at pH 9 (ca. 60 % total copper). The last three deprotonation steps lead to $[Cu(LH_{-1})]$, $[Cu(LH_{-2})]^-$ and $[Cu(LH_{-3})]^{2-}$ and they involve solely the deprotonation of the lysine residues. The coordination environment of copper in $[Cu(LH)]^{2+}$ and $[CuL]^+$ (Scheme 1) are proposed on the basis of visible absorption and CD spectra of the copper(II) / R1 (LH) system at different pH (Figure 3; UV CD spectra are reported in Figure S1).

The two spectra at pH 6.70 and 7.30, where $[Cu(LH)]^{2+}$ is predominant, exhibit an absorption λ_{max} of ca. 584 nm. By means of the parameters of the average environment (Billo's method)[49-51] this wavelength is very well accounted for the presence on the equatorial plane of copper(II) of one imidazole nitrogen, two deprotonated peptide nitrogen atoms and a water molecule (Scheme 1, left; expected λ_{max} = 583 nm).[49-51] A 6-membered chelate ring is obtained in the hypothesis of coordination of the imidazole N^δ and of the deprotonated peptide nitrogen of His268. By increasing the pH from 7.3 to 9.1 the maximum of the ligand field transition shifts from 584 to 523 nm in correspondence with the formation of $[CuL]^+$ (Figures 2 and 3).
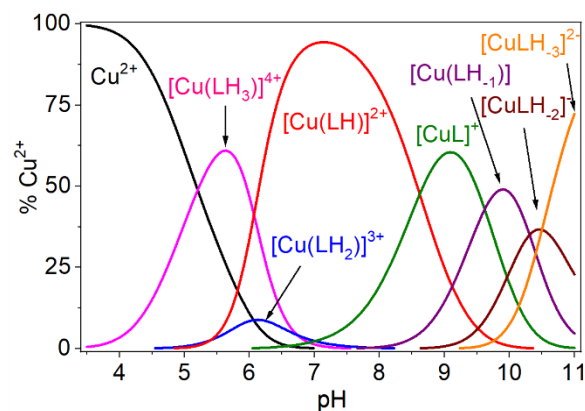

Figure 2. Representative distribution diagram of the copper(II) / R1 (LH) system in aqueous solution (Cu²⁺:R1 = 1:3, C_{Cu} = 0.47 mM, I = 0.1 M (KCl), T = 298.2 K).
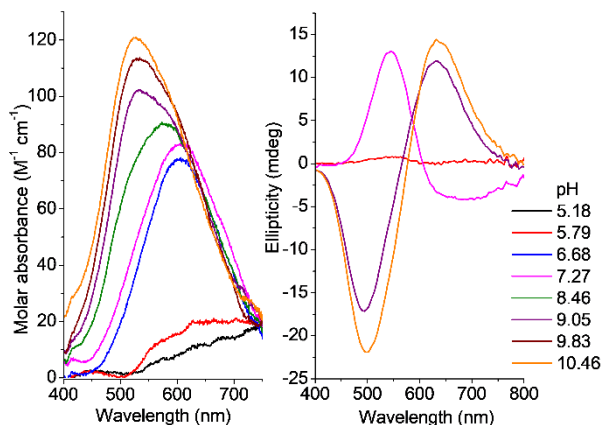
Figure 3. Left: Visible absorption spectra (Absorbance / C_{Cu}) of solutions of copper(II) and R1 (Cu²⁺:R1 = 1:1.5, C_{Cu} = 0.39 mM, I = 0.1 M (KCl), T = 298.2 K). Right: Visible CD spectra of solutions of copper(II) and R1 (Cu²⁺:R1 = 1:1.5, C_{Cu} = 0.52 mM, I = 0.1 M (KCl), T = 298.2 K).

The latter absorption maximum is very well accounted for by the presence in [CuL]⁺ of one imidazole and three peptide nitrogen atoms on the equatorial plane of copper(II) (expected λ_{max} = 523 nm).

This coordination mode is confirmed by EPR spectroscopy in which the complex between copper(II) and R1 in slight excess displays a typical axial spectrum with with magnetic parameters: $A_{\parallel}$ = (174±1) × 10⁻⁴ cm⁻¹, $A_{\perp}$ = 9±1 × 10⁻⁴ cm⁻¹, $g_{\parallel}$= 2.22±0.001 and $g_{\perp}$ = 2.055±0.0005. (Figure S2). The simulation allows to assign 3N atoms in the coordination sphere of Cu(II). Reporting the magnetic parameters into the Peisach and Blumberg diagrams in which $g_{\parallel}$ and $A_{\parallel}$ are plotted for different coordination of model Cu(II) compounds,[52] it is evident that the parameters of the R1 EPR spectrum are in agreement to a 3N coordination, confirming the assignment obtained by simulation. A schematic representation of the proposed coordination mode is reported in Scheme 1 (right).

Copper(II)/R3 complex formation equilibria. In the presence of copper(II) and in excess of ligand with respect equimolar metal:ligand ratio, the R3 peptide forms six complex species. Similarly to what observed for R1, all correspond to 1:1 copper:peptide stoichiometries. The specia-

tion model is reported in Table 1, and a representative distribution diagram is reported in Figure 4. The formation of copper:ligand 1:2 species was examined carefully for this ligand since the presence of two imidazoles may favor these stoichiometries. The fitting analysis suggests negligible formation of 1:2 species under our experimental conditions. A complete discussion of the speciation of the system is reported as a Supporting Information.

At neutral pH (pH 7-7.5) the [CuL]²⁺ and [Cu(LH₋₁)]⁺ species predominate (Figure 4). At pH 6.7, where [CuL]²⁺ is 48% of the total copper, the maximum of absorption of the *d-d* band is 610 nm. Copper(II) in this species likely adopts an equatorial (3N,O) coordination mode that involves one deprotonated peptide nitrogen, two imidazole donors, and a water molecule (Scheme 2). The expected λ_{max} for this coordination environment is 604 nm. Moving to pH 7.8 where [Cu(LH₋₁)]⁺ dominates, the spectrum of the solution experiences a blue shift to 585 nm (Figure 5; UV CD spectra are reported in Figure S3). This wavelength is well accounted for a (N_{Im}, 2N⁻, O) donor set. We have also performed EPR experiments at both pH 6.7 and 7.9 in the presence of a slight excess of R3 compared to copper(II). At pH 6.7 [CuL]²⁺ is the expected predominant species, whereas at pH 7.9 [Cu(LH₋₁)]⁺ is the most abundant. In both cases, the spectra are characteristic of an axial geometry around the metal centre (Figure S4 and S5), but severe broadening of the signal due to aggregation effects prevents reliable simulation and calculation of the magnetic parameters.
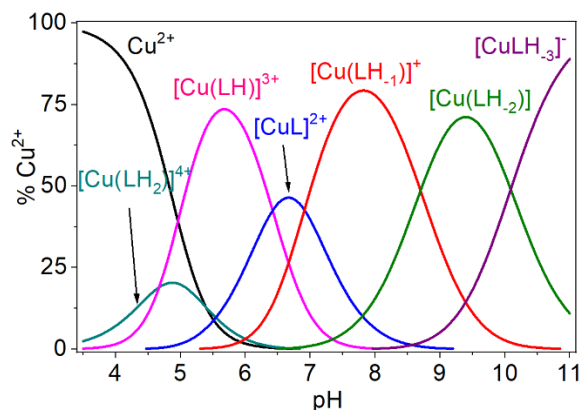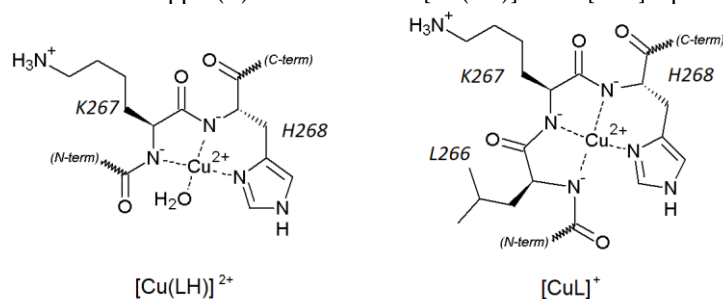

Figure 4. Representative distribution diagram of the copper(II) / R3 (L) system in aqueous solution (Cu²⁺:R3 = 1:3, C_{Cu} = 0.47 mM, I = 0.1 M (KCl), T = 298.2 K).

Scheme 1. Schematic representation of the copper(II) coordination in [Cu(LH)]²⁺ and [CuL]⁺ species of R1 (LH).
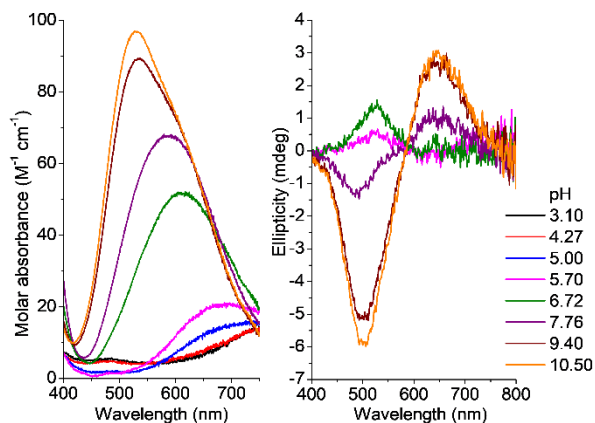

4

Figure 5. Left: Molar visible absorption spectra (Absorbance / C_{Cu}) of solutions of copper(II) and R3 (Cu^{2+}:R3 = 1:1.25, C_{Cu} = 0.60 mM, I = 0.1 M (KCl), T = 298.2 K). Right: Visible CD spectra of solutions of copper(II) and R3 (Cu^{2+}:R3 = 1:3, C_{Cu} = 0.51 mM, I = 0.1 M (KCl), T = 298.2 K).

For this coordination environment we propose chelation models that are reported in Scheme 2 (modes *a* and *b*). In the first (mode *a*) the imidazole of His329 acts as the anchor and the donor atom set is made by two deprotonated peptide nitrogen donors (Ile328 and His329) and one water molecule on the equatorial plane. In the second (mode *b*) imidazole of His 330 is the anchor, while the two-deprotonated peptide nitrogen atoms are those of (His329 and His330). For each of the two donor atom set the expected maximum of absorption calculated using the rule of the average environment (Billo's rule) is 583 nm, in full agreement with experimental 585 nm.

^{1}H-NMR data collected on R3 (see below) show how the proton signals of the Ile328-Pro332 are completely washed out upon addition of copper(II) to the peptide at neutral pH. These data suggest that possibly both modes *a* and *b* are present in solution. As for the coordination of the second imidazole, our data do not provide information on the occurrence of this interaction.

The proposed equatorial coordination modes in [Cu(LH$_{-1}$)]$^+$ start from one imidazole (either His 329 or 330) and extends toward the N-terminal. In this circumstance a stable

6-membered (N_{Im}, N^-) chelation ring is formed. An alternative coordination mode for the (N_{Im}, 2N^-, O) donor set have been proposed in the literature, and it involves the anchoring to the imidazole and the deprotonation of amides toward the C-terminal.[53, 54] For R1 and R3 peptide these coordination modes are prevented by the presence of the proline residue.

Overall, these data suggest that [CuL]$^{2+}$ and [Cu(LH$_{-1}$)]$^+$ markedly differ in their coordination environment since two imidazoles are coordinated in the equatorial plane in the former, while only one is found equatorially coordinated in the latter. This major change in the coordination of copper(II) is consistent with the major changes in the CD spectra that were observed in the pH range 6.7-7.8 (Figure 5). Here we see that the CD trace at pH 6.7 (green trace) has similar trend as the CD spectrum of copper(II):R1 at pH 7.3 (Figure 3), but the sign of the curve is inverted at pH 7.8 (violet trace). We can attribute this CD change to conformational inversion of the six-membered histidine chelate ring occurring upon binding of the axial ligand in [Cu(LH$_{-1}$)]$^+$, as this effect has been observed systematically for a number of copper(II) complexes with histidine-containing multidentate ligands.[55-57] The much stronger CD activity observed in the visible range at high pH for both Cu^{2+}:R1 and Cu^{2+}:R3 complexes cannot be attributed to vicinal or conformational effects, and is probably due to coupling of transition moments of d-d transitions with the three strong π(amide)-copper(II) charge transfer bands in the near-UV. In the literature a (3N,O) binding mode at pH 7.4 for copper(II) with several model peptides of R1 and R3 was proposed.[34] For some of these peptides the precise coordination environment was not clarified, and the involvement of the peptide groups was proposed to occur through the oxygen atom. Moreover, most of those peptides are not acetylated at their *N*-terminus and, as a consequence, the N-terminal amino group has been proposed as one of the donor groups, especially on the basis of the EPR fingerprints.[34, 58] While the coordination modes we propose agree with those in the literature for the presence of (3N,O) binding modes for both peptides at neutral pH, the major difference with the latter models is that the peptide groups are coordinated through the deprotonated nitrogen atoms, and that possibly water is the oxygen donor.[31-34]

Scheme 2. Schematic representation of the copper(II) coordination in [CuL]$^{2+}$, and [Cu(LH$_{-1}$)]$^+$ species of R3 (L).
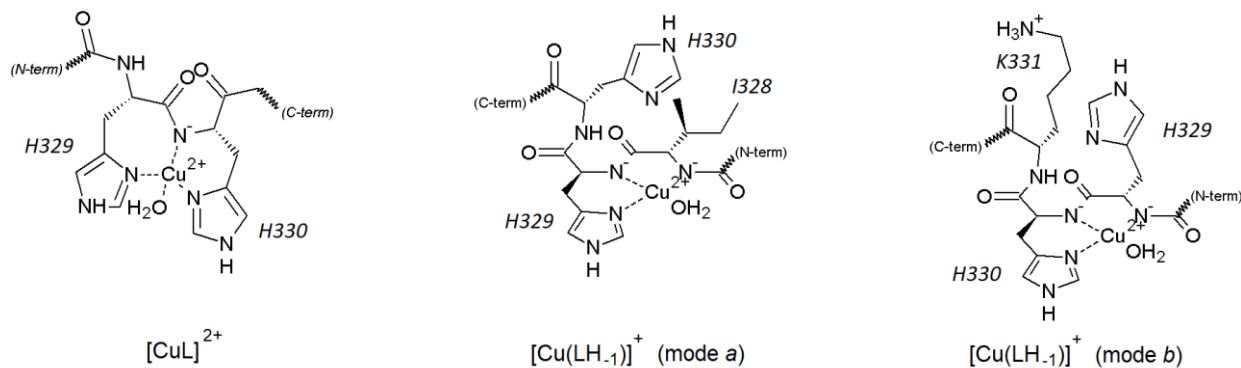
With the speciation of the two copper(II)/R1 and copper(II)/R3 systems available, we could calculate for both peptides the conditional affinities for copper(II) at pH 6.5 and at pH 7.4 (K_d for the equilibrium [CuL] = Cu + L). These two pH values are those for which the K_d of copper(II)-tau and the copper(II)/(I)-tau reduction potential are available, respectively. The K_d of the copper(II) adducts with the peptides at pH 7.4 resulted 150(10) nM for R1 and 71(5) nM for R3. Although these two values allow to calculate the copper(II)/(I)-tau reduction potentials at this pH (see below), the affinities at pH 6.5 are needed to compare with that of tau.

The conditional K_d at pH 6.5 resulted 13(1) µM for R1 and 2.8(5) µM for R3, respectively. Although these conditional affinities for copper(II) are lower than that determined for tau by ITC (500-700 nM),[30] that of R3 stays within a factor of 4 to 6 to that of the protein. It is therefore evident that a full-length tau plays a role in modulating on the overall formation constants of the copper(II)-peptide adducts that is not modelled by the fragments used in this study.

As expected, the R3 peptide has higher affinity for copper(II) than R1 at both pH values as a consequence of the presence of two His donors. However, the affinity of R3 is only 2-fold higher than that of R1 at pH 7.4, and 5-fold at pH 6.5 therefore showing that R3 is not selective in binding copper at both pH values. This is illustrated by the calculated competition diagram reported in Figure S6, which represents a hypothetical system where copper(II), R1 and R3 are present in equimolar amount as it occurs in tau protein. The relative amount of copper(II) bound to the R3 and R1 respectively is 65 vs. 35% at pH 6.5 and 58 vs. 42% at pH 7.4. Therefore, the presence in tau of one His (R1, R2 and R4 of tau) or a His-His tandem (R3) the nature of the individual sequences may not be discriminant in defining a unique binding site for copper(II). The metal in tau may rather be distributed over multiple sites, or likely be bound to one preferential site as the consequence of additional structural features not modelled using R1 and R3 peptides.

Copper(I)/R1 and copper(I)/R3 complex formation equilibria. The formation constants of copper(I) complexes with R3 was determined in aqueous 4-(2-hydroxyethyl)-1-piperazine ethanesulfonic acid (HEPES) buffer 100 mM at pH 7.4. As a consequence of the use of the buffer, these are apparent constants. However, there is consensus in the literature for not considering HEPES as a strong competing ligand for copper(I).[59] We expect therefore the values of these apparent formation constants to be not significantly different to conditional ones. UV-visible competition experiments were carried out using ferrozine (Fz²⁻) as a competing metallochromic indicator for copper(I). By adding R3 to a [Cu(Fz)₂]³⁻ solution, a decrease in the absorbance values in the range 450-800 nm was observed as a consequence of copper(I) displacement from the indicator (Figure 6).
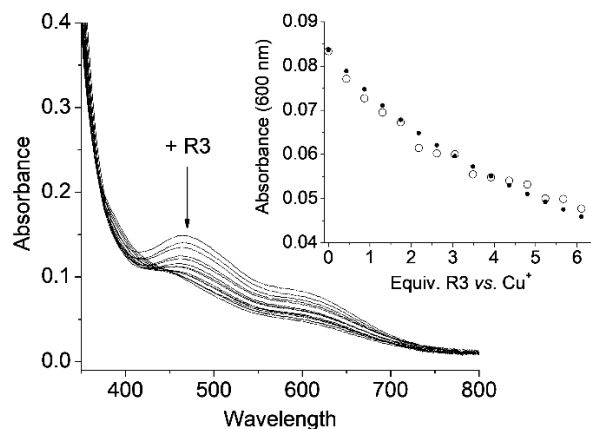

Figure 6. Spectral dataset for the titration of a solution of [Cu(CH$_3$CN)$_4$]BF$_4$ and Fz²⁻ with R3 (Cu:Fz = 1:2.15, C_{Cu} = 41 µM, $C_{ascorbate}$ = 10 mM, 100 mM aqueous HEPES buffer solution, pH 7.4). Insect: absorbance values at 600 nm. Open circles: observed; filled circles: calculated.

Conversely, the limited decrease in absorbance observed with R1 was fully accounted by dilution effects, which suggests that the formation log β value of a possible copper(I)/R1 adduct is lower than 5 (see Figure S7). Data treatment of the spectral dataset for the titrations with both peptides allowed to calculate the conditional log β values for the Cu⁺ + L = [CuL] equilibria, which resulted 10.1(2) for R3 (corresponding to a dissociation constant of 7.9 10⁻¹¹ M) and not significant for R1.

Overall, all these data confirm that the R1 peptide does not bind significantly copper(I), while the R3 peptide has a high affinity for copper(I). This result was not unexpected, since previous investigations of histatin peptides and models of Aβ and Ctr1 has proven the affinity of His-His tandem for copper(I).[59-62] For these peptides affinities in the range of 10⁻¹⁰-10⁻¹¹ M were reported, although affinities down to 10⁻⁶ M have been reported.[59-62] As for the coordination environment, we put forward the hypothesis that the main binding site is at the two imidazole groups of His 329 and His 330: copper(I) is likely (N_{im},N_{im}) two-coordinated with a possible weak interaction of the carbonyl oxygen of His 329. The involvement of the imidazole groups as the donor ligands is in full agreement with NMR data (see below). Finally, in the attempt to exclude a buffer competing effect that could bias the comparison with NMR data, we have performed the same competition experiments in 100 mM phosphate buffer at pH 7.0. Formation constants are not significantly different from those in HEPES (not shown).

Structural characterization of copper-R3 complexes by NMR spectroscopy. Copper(II) and copper(I) binding to R3 at pH 6.8 was also investigated by NMR spectroscopy. Upon addition of the paramagnetic ion to R3 solutions, we observed selective line broadening of NMR resonances. As shown in Figure 7, the most affected signals were those belonging to His329, His330 and residues nearby, Ile328, Lys331 and Pro332. As usually found for copper(II)-peptide interactions, the higher is the metal concentration the
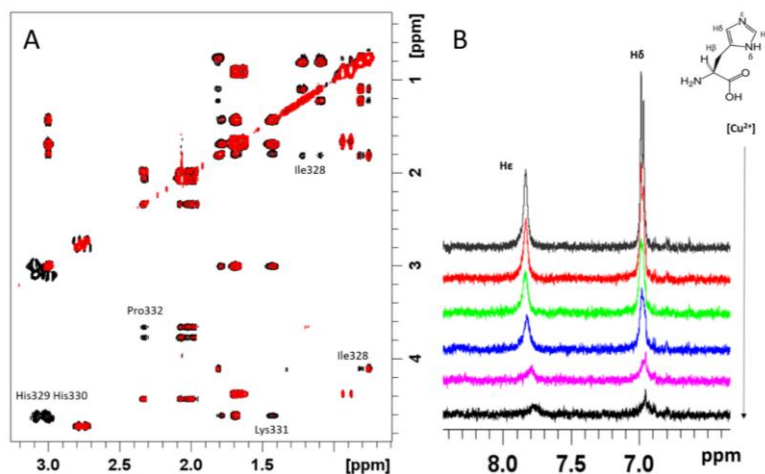
Figure 7. A. Comparison of selected region of ¹H-¹H TOCSY spectra of R3 in absence (black contours) and in presence (red spots) of 0.2 equivalents of copper(II). B. Superimposition of ¹H 1D NMR spectra of apo R3 both free (upper trace) and in the presence of increasing copper(II) concentration.

larger is the metal induced line broadening of NMR signals, as shown in Figure 7B. The most affected protons are those belonging to His imidazole rings, Hδ and Hε. In particular, the effects are more pronounced on Hε than Hδ, indicating Nδ rather than Nε, as binding donor atom for both His.[63-65] Besides copper(II), we also investigated copper(I)-R3 association. Copper(I) is diamagnetic and it induces chemical shift variations of protein/peptide nuclei close to the metal coordination sphere. As it is evident from Figure 8, signals of both His329 and His330 are downfield shifted supporting their binding to the cuprous ion.[66, 67] Moreover, Figure 8 shows changes on Ile328 methyl protons as well, this might be explained by considering their proximity to the metal center. Similar effects were obtained by using Ag(I) as copper probe. In this case, Ag(I) causes upfield shift of

His protons, in agreement with what we recently reported on copper(I) interaction with Aβ peptides.[66] This similar behavior is consistent with the fact that a His-His tandem is present in Aβ as well as in R3 and it plays a key role in metal interactions.[68, 69]

The interaction between copper(II) and R1 has been also investigated by NMR spectroscopy. Both ¹H 1D and ¹H-¹H TOCSY NMR spectra (Figure S8) indicate that the presence of copper(II) induces large broadening of the signals of His268 and of the vicinal residues (Leu266, Gln269 and Pro270). These data confirm the relevance of His268 as anchoring site for the coordination of copper(II).
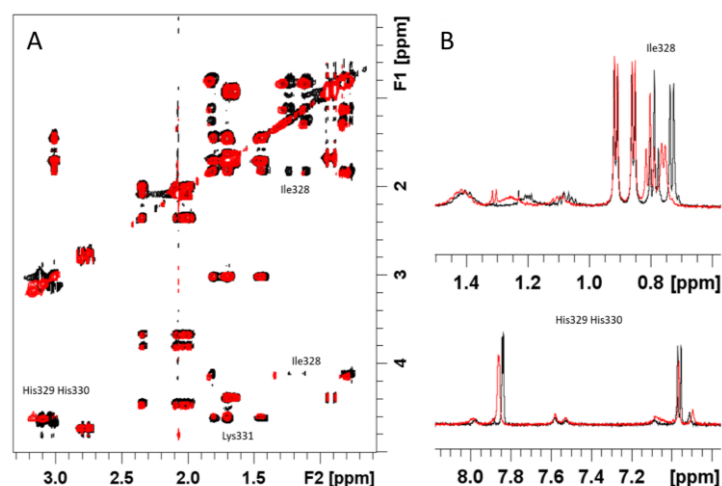

Figure 8. A. Comparison of selected region of ¹H-¹H TOCSY spectra of R3 in absence (black contours) and in presence (red spots) of 0.8 equivalents of copper(I). B. Superimposition of ¹H 1D NMR spectra of apo R3 both free (black trace) and in presence (red trace) of 0.8 equivalents of copper(I).

7

Oxidation of dopamine and 4-methylcatechol by copper-R1 and copper-R3 complexes. To gain information on the potential catalytic role of copper-R1 and -R3 complexes in oxidative reactions, we performed a comparative study of their oxidative activity against catecholic substrates with respect to that of free copper(II). The most important substrate that can be involved in this type of reactivity is DA, due to its abundance in *substantia nigra* neurons and because alteration in DA metabolism can be related to several neurodegenerative disorders.[70] Catecholamines are present in many brain areas besides the substantia nigra, and in particular in those regions which are mostly affected by AD and Parkinson's disease.[71]

The oxidation of DA catalyzed by copper(II) in HEPES buffer at pH 7.4 was studied in the presence of increasing amounts of either R1 or R3, in parallel experiments. DA oxidation was monitored by UV-visible spectroscopy through the development of the absorption band of dopaminochrome (DAC) at 475 nm. This product accumulates in the initial stages of the reaction.[72, 73] Within about 1 h, formation of insoluble melanic products could be noted; therefore, we focused our attention on the first 30 min of reaction. In these conditions, DA autoxidation is not negligible, as shown by the black dotted trace in Figure 9. DA (3 mM) oxidation catalyzed by copper(II) (25 μM) is strongly promoted by the addition of R3 but it is only slightly enhanced by the presence of R1. In both cases, the DA oxidation increases by increasing the tau/copper(II) ratio.

Since DA oxidation is rather slow and occurs with formation of mixture of products and precipitate, this substrate is not suitable to perform a more detailed kinetic study. Therefore, the oxidation of the more reactive MC (with a lower semiquinone/catechol redox potential)[46] can be conveniently studied as a model substrate of DA. Oxidation of MC (3 mM) promoted by copper(II) (25 μM) and tau peptides at pH 7.4 (50 mM HEPES buffer) proceeds with a biphasic behavior where a fast initial step, concluded after about 100 s, is followed by a second linear phase (Figure 10).

The biphasic behavior can be noted also for DA oxidation but the presence of several absorbing species in solution makes the observation less clear. During the time course of MC oxidation, a shift of the developing absorption bands occurs from the initial value of 401 nm, due to the 4-methylquinone (MQ), to higher wavelengths, which is related to the formation of the quinone addition product with catechol.[47] By increasing the peptide concentration, the rate of both steps is accelerated with a much stronger effect observed in the presence of R3 rather than the complex with R1.
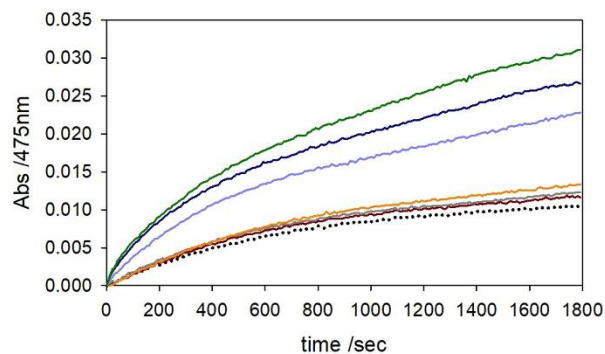

Figure 9. Kinetic profile of DA (3 mM) oxidation with time in 50 mM HEPES buffer solution at pH 7.4 and 20 °C in the presence of only copper(II) (25 μM) (brown trace) and with 2 equiv. (grey), 4 equiv. (orange) of R1 peptide or 1 equiv. (light blue), 2 equiv. (blue) and 4 equiv. (green) of R3. Autoxidation of substrate is also shown (black dotted trace).

Figure 10. Kinetic profile of MC (3 mM) oxidation with time in 50 mM HEPES buffer solution at pH 7.4 and 20 °C in the presence of only copper(II) (25 μM) (brown trace) and with 2 equiv. (grey), 4 equiv. (orange) of R1 peptide or 1 equiv. (light blue), 2 equiv. (blue) and 4 equiv. (green) of R3. Autoxidation of substrate is also shown (black dotted trace).
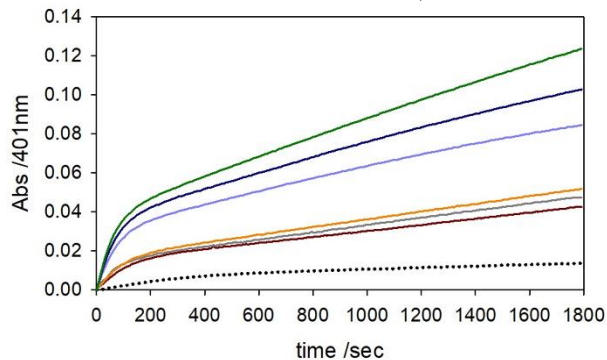
Prior to analyse the reaction mechanism and compare the different behaviour in the presence of the two peptides, we could estimate the reduction potential of the copper(II)/(I) couple by using the formation constants of copper(I) and copper(II) complexes with the two peptides. As for the copper(I)/R1 adduct, for which a log β value could not be determined, an upper limit of log β = 5 was considered (see above). With these data in our hands, we could estimate a reduction potential of -170(10) and +110(10) mV vs. NHE for R1 and R3, respectively. The former value (-170 mV for copper/R1) represents an upper limit under our approximations.

It was previously demonstrated that the presence on peptide sequences of tandem His-His sites promotes the reduction of copper(II) to copper(I), mainly through the formation of stable copper(I)/peptide adducts.[59-62] It is however worth noting that here for both R1 and R3 fragments the estimated potential is lower than that observed for copper adducts with tau (340 mV vs. NHE).[38] Assuming for R3 and tau a similar affinity for copper(I), the difference of an

order of magnitude in the affinities for copper(II) accounts only for 60 mV of the difference in their redox potentials. Overall these data suggest that there are structural or second-shell interactions in copper/tau adducts that determine the redox potential in the protein and that are not completely modelled by R1 and R3 peptides.

The reaction mechanism previously proposed for the oxidation of catechols by copper-Aβ,[43] copper-α-synuclein[46] and copper-prion[48] peptide complexes can be extended to the present study on copper-tau peptide complexes. It involves the following reaction steps:

1. Cu^{2+} + peptide $\rightleftarrows$ [Cu^{2+}-peptide]
2. [Cu^{2+}-peptide] + catechol $\rightarrow$ [Cu^+-peptide] + semiquinone$^{\bullet+}$
3. [Cu^+-peptide] + catechol $\rightleftarrows$ [Cu^+-peptide-catechol]
4. [Cu^+-peptide-catechol] + O_2 $\rightarrow$ [Cu-peptide-catechol-O_2]
5. [Cu-peptide-catechol-O_2] $\rightarrow\rightarrow$ [Cu^{2+}-peptide] + quinone

After rapid complexation (reaction 1), the reaction proceeds with the reduction of copper(II) to copper(I) by the catechol, which occurs as a fast phase (reaction 2). The rate-determining step is reaction 4 of the reduced form of Cu-peptide complex with dioxygen, to generate the ternary complex indicated as [Cu-PrP-catechol-O_2]. Our previous studies on copper-peptide complexes indicate that the reaction rate depends also on catechol concentration, suggesting that substrate binding occurs as a pre-equilibrium step before the rate-determining binding of molecular oxygen.[43, 46, 48] The R3 binding to copper(I) facilitates the reaction with molecular oxygen, increasing the reaction rate (Figures 9 and 10). On the other hand, the weak affinity towards R1 leaves copper(I) mostly unbound to the peptide and, thus, with a reactivity comparable with that observed for "free" copper (Figures 9 and 10). The presence of the catechol, which could bind to the metal ions, could complicate the scenario, perturbing the binding processes. Anyway, the activity data clearly indicate that the turnover reactivity of the copper/peptide complexes is controlled by the copper(I) binding mode, confirming the key role of His-His tandem in R3 fragment. An increase of the rate of copper-mediated oxidation of catecholic substrates has been already observed in the presence of Aβ[43, 74, 75] and prion protein[48] fragments, whereas truncated α-synuclein peptides induce a decrease in the reactivity of copper.[46] This behavior suggests that the multiple histidine residues present in Aβ, prion protein and R3 peptides, but not in R1 and α-synuclein, are crucial for this reactivity.

Conversely, in the presence of other substrate as ascorbate the rate of oxidation is higher with copper compared to that of copper-Aβ[76, 77] or copper-α-synuclein[45] peptide complexes. This behavior can be ascribed to the different coordination properties of different substrate for copper in both oxidation states and to a possible change in the rate limiting step of the overall process.

Competitive endogenous R1 and R3 peptide oxidation. Similarly to our previous studies on other copper-peptide complexes,[43, 46, 48] we investigated the metal-catalyzed oxidation of tau peptides in the reductive environment generated during catechol oxidation, by using LC-MS analysis.

This aspect is important because, unlike copper enzymes that activate oxygen for specific reactions,[78] copper complexes with neuronal peptides generate Cu/O_2 species capable of non-selective oxidations. This reactivity is due to Fenton chemistry yielding harmful reactive oxygen species (ROS) that give rise to oxidative protein damage, through oxidation of amino acid residues, structural alteration and loss of function.[79-82] These reactions contribute to the oxidative damage observed in AD, especially addressed to Aβ,[83] but they can also reasonably involve tau protein. In this LC-MS analysis, the oxidative modifications on R1 and R3 peptides produced upon oxidation of both DA and MC were evaluated. In these experiments, a solution of copper and tau peptides was incubated in the presence of DA or MC in the same conditions as in the catalytic oxidations ([tau peptide] = 50 μM; [Cu^{2+}] = 25 μM; [catechol] = 3 mM; in 50 mM HEPES buffer pH 7.4). Samples were analysed after 15, 30 and 90 min reaction time.

R1 fragment undergoes a limited pattern of modifications in the presence of MC (Figure 11 – panel A), whereas in the presence of DA the peptide remains mostly unmodified (peak with t_R = 26 min, Figure 11 – panel B). In the latter case, the peak appearing at t_R of 24 min, with relative area of 7 %, is not corresponding to an oxidative modification but it is probably due to a fragmentation derivative.
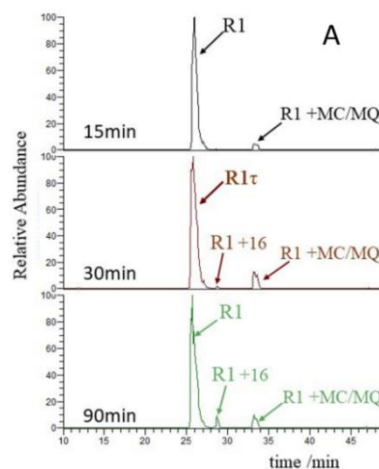

9

Table 2. Modification of R1 peptide (50 µM) detected by LC-MS analysis, in the presence of copper(II) (25 µM) and MC or DA (3 mM) in HEPES buffer (50 mM) pH 7.4 at 20 °C.

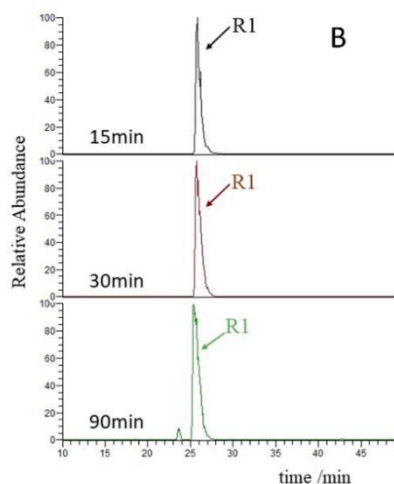| Incubation time (min)	R1	+16	+MQ	+MC	+MQ +16	+MC +16
15	95%	-	3%	2%	-	-
30	88%	1%	6%	5%	-	-
90	85%	3%	5%	5%	1%	1%
Incubation time (min)	**R1**	**+16**	**+DAQ**	**+DA**	**+DAQ +16**	**+DA +16**
15	100%	-	-	-	-	-
30	100%	-	-	-	-	-
90	93%	-	-	-	-	-

Figure 11. HPLC-MS elution profiles of R1 peptide (50 µM) in HEPES buffer (50 mM) pH 7.4 in the presence of copper(II) (25 µM) and MC (panel A) or DA (panel B) (3 mM) after 15, 30 and 90 min reaction time.

Table 2 reports the variation over time of the percent modification of the native peptide. These data show that in the presence of MC the most abundant modification underwent by R1 peptide is the nucleophilic addition of MC and MQ to His residue (two adjacent peaks with t_R = 33/34 min). The modification that implies an oxygen atom insertion (R1+16, peak with t_R = 29 min) is limited and it is only observed in low amount after prolonged incubation (1 % after 30 min and 3 % after 90 min).

The oxidative modifications of R3 peptide are larger both in terms of the number of products and in terms of the extension of the modifications (Figure 12). In the presence of DA (Figure 12 – panel B), the most abundant modification corresponds to the peak with mass increment of +16 (t_R = 27 min) that indicates the insertion of an oxygen atom (11 % after 30 min and 29 % after 90 min – Table 3). It is possible to note also the double insertion of oxygen (+32 total mass increment – 8 % after 90 min), whereas small amount of derivatives obtained from addition of catechol (2 % of R3-DA+16) or quinone (1 % of R3-DAQ and 2 % of R3-DAQ+16) even after 90 min are observed.

In the presence of MC, the pattern of modification is even more complicated (Figure 12 – panel A). The types of modification identified by LC-MS analysis include: (i) O-atom insertion into His329 or His330 (+16 mass increment); (ii) double O-atom insertion into both His residue (+32); (iii) addition of MQ to one His residue (+120); (iv) addition of MC to one His residue (+122); (v) a double modification consisting in MQ addition to one His residue (+120) and O-atom insertion into His (+16), yielding a total mass increment of 136; (vi) a double modification consisting in MC addition to one His residue (+122) and O-atom insertion into His (+16), yielding a total mass increment of 138; (vii) oxidation of Pro332 to hydroxyproline[84] followed by dehydration (mass loss of 2).Contrarily to the data regarding R1 in which the nucleophilic addition was predominant, in

Table 3. Modification of R3 peptide (50 µM) detected by LC-MS analysis, in the presence of copper(II) (25 µM) and MC or DA (3 mM) in HEPES buffer (50 mM) pH 7.4 at 20 °C.

Incubation time (min)	R3	-2	+16	+16 +16	+MQ	+MC	+MQ +16	+MC +16
15 min	40%	5%	27%	13%	1%	1%	6%	7%
30 min	23%	8%	36%	11%	1%	2%	7%	12%
90 min	8%	12%	36%	18%	1%	2%	7%	16%
Incubation time (min)	**R3**	**-2**	**+16**	**+16 +16**	**+DAQ**	**+DA**	**+DAQ +16**	**+DA +16**
15 min	97%	-	3%	-	-	-	-	-
30 min	86%	-	11%	3%	-	-	-	-
90 min	53%	4%	29%	8%	1%	-	2%	2%

this case the oxygen insertion is the most abundant modification.

In conclusion, R3 undergoes extensive modifications, since the amount of unmodified peptide is only 8 % after 90 min of time incubation. The LC-MS data are in agreement with the catalytic data on catechol oxidation. R1 fragment is weakly bound to copper(I), leading to a slow reaction with molecular oxygen and thus to weak catalytic activity in catechol oxidation and limited "self-modification".
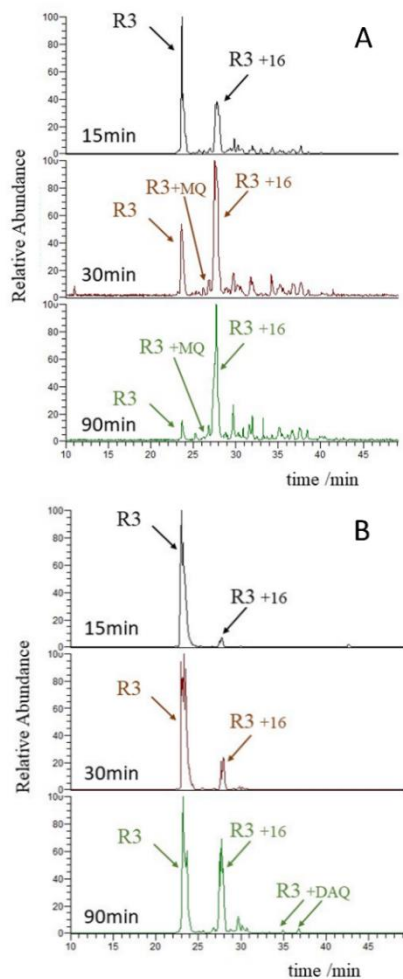

Figure 12. HPLC-MS elution profiles of R3 peptide (50 μM) in HEPES buffer (50 mM) pH 7.4 in the presence of copper(II) (25 μM) and MC (panel A) or DA (panel B) (3 mM) after 15, 30 and 90 min reaction time.

It is also possible to compare the tendency to undergo copper-mediated oxidative modification of tau R3 and R1 peptides with other neuronal peptides analysed in the same experimental conditions in previous studies by our group. By considering the percentage of unmodified peptide after 90 min in the presence of copper and MC it is possible to list the neuronal peptides in this order of reactivity: R3 > prion fragment 76-114 (PrP$_{76-114}$)[48] > Aβ16 ≈ Aβ28[43] >> R1 > α-synuclein fragment 1-15.[46]

SOD-like reactivity of copper-R1 and copper-R3 complexes. We also measured the SOD-like activity of copper(II)-R1 and copper(II)-R3 complexes in comparison to the activity of free copper(II) in solution. The activity was evaluated through the direct assay in which O_2^- is supplied as KO_2-crown ether complex, as we reported previously for copper(II)-prion,[48] copper(II)-Aβ[44] and copper(II)-α-synuclein[46] peptide complexes. As shown in Figure S9, neither copper(II)-R1, nor copper(II)-R3 significantly increase the SOD activity of free copper(II).

CONCLUSIONS

Compared to the interaction of copper with other neuronal peptides involved in the pathogenesis of neurodegenerative diseases, which has been deeply elucidated, the interaction of copper with tau protein is poorly characterized, even if the relevance and the impact of tau homoeostasis in neurodegenerative diseases progression is taking a central stage in the last years. The present study presents a thorough and detailed analysis of the stability and the structural models of copper (in both oxidation states) complexes with two peptide fragments that are encompassed in the R1 and R3 repeats of tau.

Potentiometric measurements suggest that the vicinal His-His residues in R3 guarantees a strong binding site for copper in both oxidation states (K_d value of 71 nM and 0.08 nM for copper(II) and copper(I), respectively), whereas the single histidine in R1 can bind copper(II) (K_d = 150 nM) but not copper(I). CD and NMR techniques confirm the involvement of the His-His tandem in the coordination of copper in both oxidation state.

The study of the oxidative reactivity of these copper-tau peptide complexes confirms that R3 coordination sphere guarantees an efficient copper(I)/(II) redox cycling. In particular, copper-R3 complex is able to strongly enhance the capability of copper to oxidize cathecolic substrates as DA and MC, whereas copper-R1 complex reactivity is similar to that of free copper. The reduction of copper during the catechol oxidation generate Cu/O_2 species capable to oxidize other cellular components through Fenton chemistry. LC-MS analysis of the reaction mixture indicate that R3 is rapidly and extensively modified, through oxygen insertion and/or quinone-derivatized histidines. By comparing the tendency to undergo copper-mediated oxidative modification of tau R3 and R1 peptides with other neuronal peptides analysed in previous studies by our group we can conclude that R3 is the most reactive, followed by prion protein fragment (PrP$_{76-114}$) and N-terminal portion of Aβ peptide.

In conclusion, the His-His tandem strongly discriminates the copper binding rendering the copper(I) coordination more favourable in R3 compared to R1. This site accommodates copper in both oxidation states providing an active catalyst for reactions that activate oxygen and are potentially dangerous for the cellular compartment. The different binding of copper(I) for R3 and R1 fragments is particularly important for this interaction because tau protein is

located intracellularly where the reductive redox potential implies that copper is mostly in the reduced state.

The next steps of this bottom-up approach for deciphering the copper-tau interaction might include: (i) the study of the copper complex with R3 peptide that includes the cysteine residue, which has a relevant role in tau aggregation; (ii) the analysis of protein fragments that contain more than one copper binding site in order to understand if the individual binding site is influenced by each other's; (iii) once characterized the individual binding site for copper, the extension of the study to full length protein; (iv) the implementation of this *in vitro* approach by introducing other cellular components such as membrane-like environment.

ASSOCIATED CONTENT

Supporting Information. Materials and methods, detailed description of copper complexes formation equilibria, EPR spectra, additional CD and UV-visible spectra. This material is available free of charge via the Internet at http://pubs.acs.org.

AUTHOR INFORMATION

Corresponding Author

matteo.tegoni@unipr.it

simone.dellacqua@unipv.it

ORCID id

Chiara Bacchella: 0000-0003-3256-8699

Silvia Gentili: 0000-0001-9323-0283

Denise Bellotti: 0000-0002-2634-0228

Daniela Valensin: 0000-0003-4187-3919

Enrico Monzani: 0000-0002-8791-6446

Maurizio Remelli: 0000-0002-5705-3352

Stefania Nicolis: 0000-0002-6618-7555

Luigi Casella: 0000-0002-7671-0506

Matteo Tegoni: 0000-0002-9621-0410

Simone Dell'Acqua: 0000-0002-1231-4045

Author Contributions

C.B, preparation and purification of the peptides; acquisition and analysis of kinetic and HPLC-MS experiments. S.G., acquisition and analysis of potentiometric, spectrophotometric and CD data. D.B., acquisition and analysis of potentiometric and spectrophotometric data. E.Q., acquisition and analysis of potentiometric, spectrophotometric and CD data. S.D., acquisition and analysis of NMR experiments. M.R., analysis and interpretation of copper(II) binding experiments; preparation of the manuscript. M.C.B. analysis and interpretation of EPR experiments. D.V., analysis and interpretation of NMR experiments; preparation of the manuscript. E.M., analysis and interpretation of kinetic experiments. S.N., analysis and interpretation of HPLC-MS experiments. L.C., conception of the project; preparation of the manuscript. M.T., conception of the project; analysis and interpretation of potentiometric, spectrophotometric and CD data; preparation of the manuscript. S.D.A., conception of the project; analysis and interpretation of kinetic experiments; preparation of the manuscript. All authors revised critically the manuscript and approved its final version.

REFERENCES

1. Weingarten, M. D.; Lockwood, A. H.; Hwo, S. Y.; Kirschner, M. W., A protein factor essential for microtubule assembly. *Proceedings of the National Academy of Sciences* **1975,** *72* (5), 1858.
2. Jeganathan, S.; von Bergen, M.; Brutlach, H.; Steinhoff, H.-J.; Mandelkow, E., Global Hairpin Folding of Tau in Solution. *Biochemistry* **2006,** *45* (7), 2283-2293.
3. Wang, Y.; Mandelkow, E., Tau in physiology and pathology. *Nature Reviews Neuroscience* **2015,** *17*, 22.
4. Spillantini, M. G.; Goedert, M., Tau pathology and neurodegeneration. *Lancet Neurol* **2013,** *12* (6), 609-22.
5. Fuster-Matanzo, A.; Hernández, F.; Ávila, J., Tau spreading mechanisms; Implications for dysfunctional tauopathies. *International Journal of Molecular Sciences* **2018,** *19* (3).
6. Masters, C. L.; Bateman, R.; Blennow, K.; Rowe, C. C.; Sperling, R. A.; Cummings, J. L., Alzheimer's disease. *Nat Rev Dis Primers* **2015,** *1*, 15056.
7. Gong, C. X.; Iqbal, K., Hyperphosphorylation of microtubule-associated protein tau: a promising therapeutic target for Alzheimer disease. *Curr Med Chem* **2008,** *15* (23), 2321-8.
8. Brister, M. A.; Pandey, A. K.; Bielska, A. A.; Zondlo, N. J., OGlcNAcylation and Phosphorylation Have Opposing Structural Effects in tau: Phosphothreonine Induces Particular Conformational Order. *Journal of the American Chemical Society* **2014,** *136* (10), 3803-3816.
9. Reynolds, M. R.; Reyes, J. F.; Fu, Y.; Bigio, E. H.; Guillozet-Bongaarts, A. L.; Berry, R. W.; Binder, L. I., Tau nitration occurs at tyrosine 29 in the fibrillar lesions of

Alzheimer's disease and other tauopathies. *J Neurosci* **2006,** *26* (42), 10636-45.

10.   Lindsley, C. W.; Hooker, J. M., Beyond the Amyloid Hypothesis of Alzheimer's Disease: Tau Pathology Takes Center Stage. *ACS Chemical Neuroscience* **2018,** *9* (11), 2519.

11.   Lippens, G.; Gigant, B., Elucidating Tau function and dysfunction in the era of cryo-EM. *J Biol Chem* **2019.**

12.   Fitzpatrick, A. W. P.; Falcon, B.; He, S.; Murzin, A. G.; Murshudov, G.; Garringer, H. J.; Crowther, R. A.; Ghetti, B.; Goedert, M.; Scheres, S. H. W., Cryo-EM structures of tau filaments from Alzheimer's disease. *Nature* **2017,** *547,* 185.

13.   Alavi Naini, S. M.; Soussi-Yanicostas, N., Tau Hyperphosphorylation and Oxidative Stress, a Critical Vicious Circle in Neurodegenerative Tauopathies? *Oxid Med Cell Longev* **2015,** *2015,* 151979.

14.   Ibanez-Salazar, A.; Banuelos-Hernandez, B.; Rodriguez-Leyva, I.; Chi-Ahumada, E.; Monreal-Escalante, E.; Jimenez-Capdeville, M. E.; Rosales-Mendoza, S., Oxidative Stress Modifies the Levels and Phosphorylation State of Tau Protein in Human Fibroblasts. *Front Neurosci* **2017,** *11,* 495.

15.   Savelieff, M. G.; Lee, S.; Liu, Y.; Lim, M. H., Untangling Amyloid-β, Tau, and Metals in Alzheimer's Disease. *ACS Chemical Biology* **2013,** *8* (5), 856-865.

16.   Leal, S. S.; Botelho, H. M.; Gomes, C. M., Metal ions as modulators of protein conformation and misfolding in neurodegeneration. *Coordination Chemistry Reviews* **2012,** *256* (19), 2253-2270.

17.   Cheignon, C.; Tomas, M.; Bonnefont-Rousselot, D.; Faller, P.; Hureau, C.; Collin, F., Oxidative stress and the amyloid beta peptide in Alzheimer's disease. *Redox Biology* **2018,** *14,* 450-464.

18.   Kepp, K. P., Bioinorganic Chemistry of Alzheimer's Disease. *Chemical Reviews* **2012,** *112* (10), 5193-5239.

19.   Valensin, D.; Dell'Acqua, S.; Kozlowski, H.; Casella, L., Coordination and redox properties of copper interaction with α-synuclein. *Journal of Inorganic Biochemistry* **2016,** *163,* 292-300.

20.   Carboni, E.; Lingor, P., Insights on the interaction of alpha-synuclein and metals in the pathophysiology of Parkinson's disease. *Metallomics* **2015,** *7* (3), 395-404.

21.   La Mendola, D.; Rizzarelli, E., Evolutionary Implications of Metal Binding Features in Different Species' Prion Protein: An Inorganic Point of View. *Biomolecules* **2014,** *4* (2).

22.   Kepp, K. P., Alzheimer's disease: How metal ions define β-amyloid function. *Coordination Chemistry Reviews* **2017,** *351,* 127-159.

23.   Kozlowski, H.; Luczkowski, M.; Remelli, M.; Valensin, D., Copper, zinc and iron in neurodegenerative diseases (Alzheimer's, Parkinson's and prion diseases). *Coordination Chemistry Reviews* **2012,** *256* (19–20), 2129-2141.

24.   Migliorini, C.; Porciatti, E.; Luczkowski, M.; Valensin, D., Structural characterization of Cu2+, Ni2+ and Zn2+ binding sites of model peptides associated with neurodegenerative diseases. *Coordination Chemistry Reviews* **2012,** *256* (1-2), 352-368.

25.   Mo, Z. Y.; Zhu, Y. Z.; Zhu, H. L.; Fan, J. B.; Chen, J.; Liang, Y., Low micromolar zinc accelerates the fibrillization of human tau via bridging of Cys-291 and Cys-322. *J Biol Chem* **2009,** *284* (50), 34648-57.

26.   Sun, X. Y.; Wei, Y. P.; Xiong, Y.; Wang, X. C.; Xie, A. J.; Wang, X. L.; Yang, Y.; Wang, Q.; Lu, Y. M.; Liu, R.; Wang, J. Z., Synaptic released zinc promotes tau hyperphosphorylation by inhibition of protein phosphatase 2A (PP2A). *J Biol Chem* **2012,** *287* (14), 11174-82.

27.   Jiji, A. C.; Arshad, A.; Dhanya, S. R.; Shabana, P. S.; Mehjubin, C. K.; Vijayan, V., Zn2+ Interrupts R4-R3 Association Leading to Accelerated Aggregation of Tau Protein. *Chemistry – A European Journal* **2017,** *23* (67), 16976-16979.

28.   Yamamoto, A.; Shin, R. W.; Hasegawa, K.; Naiki, H.; Sato, H.; Yoshimasu, F.; Kitamoto, T., Iron (III) induces aggregation of hyperphosphorylated τ and its reduction to iron (II) reverses the aggregation: implications in the formation of neurofibrillary tangles of Alzheimer's disease. *Journal of Neurochemistry* **2004,** *82* (5), 1137-1147.

29.   Pirota, V.; Monzani, E.; Dell'Acqua, S.; Casella, L., Interactions between heme and tau-derived R1 peptides: binding and oxidative reactivity. *Dalton Transactions* **2016,** *45* (36), 14343-14351.

30.   Soragni, A.; Zambelli, B.; Mukrasch, M. D.; Biernat, J.; Jeganathan, S.; Griesinger, C.; Ciurli, S.; Mandelkow, E.; Zweckstetter, M., Structural Characterization of Binding of Cu(II) to Tau Protein†. *Biochemistry* **2008,** *47* (41), 10841-10851.

31.   Zhou, L. X.; Du, J. T.; Zeng, Z. Y.; Wu, W. H.; Zhao, Y. F.; Kanazawa, K.; Ishizuka, Y.; Nemoto, T.; Nakanishi, H.; Li, Y. M., Copper (II) modulates in vitro aggregation of a tau peptide. In *Peptides*, United States, 2007; Vol. 28, pp 2229-34.

32.   Ma, Q.; Li, Y.; Du, J.; Liu, H.; Kanazawa, K.; Nemoto, T.; Nakanishi, H.; Zhao, Y., Copper binding properties of a tau peptide associated with Alzheimer's disease studied by CD, NMR, and MALDI-TOF MS. *Peptides* **2006,** *27* (4), 841-849.

33.   Ma, Q.-F.; Li, Y.-M.; Du, J.-T.; Kanazawa, K.; Nemoto, T.; Nakanishi, H.; Zhao, Y.-F., Binding of copper (II) ion to an Alzheimer's tau peptide as revealed by MALDI-TOF MS, CD, and NMR. *Biopolymers* **2005,** *79* (2), 74-85.

34.   Shin, B.-k.; Saxena, S., Insight into Potential Cu(II)-Binding Motifs in the Four Pseudorepeats of Tau Protein. *The Journal of Physical Chemistry B* **2011,** *115* (50), 15067-15078.

35.   Du, X.; Zheng, Y.; Wang, Z.; Chen, Y.; Zhou, R.; Song, G.; Ni, J.; Liu, Q., Inhibitory Act of Selenoprotein P on Cu+/Cu2+-Induced Tau Aggregation and Neurotoxicity. *Inorganic Chemistry* **2014,** *53* (20), 11221-11230.

36.   Di Natale, G.; Bellia, F.; Sciacca, M. F. M.; Campagna, T.; Pappalardo, G., Tau-peptide fragments and

their copper(II) complexes: Effects on Amyloid-β aggregation. *Inorganica Chimica Acta* **2018,** *472,* 82-92.

37.   Susanne Becker, J.; Zoriy, M.; Przybylski, M.; Sabine Becker, J., Study of formation of Cu- and Zn-containing tau protein using isotopically-enriched tracers by LA-ICP-MS and MALDI-FTICR-MS. *Journal of Analytical Atomic Spectrometry* **2007,** *22* (1), 63-68.

38.   Martic, S.; Rains, M. K.; Kraatz, H.-B., Probing copper/tau protein interactions electrochemically. *Analytical Biochemistry* **2013,** *442* (2), 130-137.

39.   Sayre, L. M.; Perry, G.; Harris, P. L.; Liu, Y.; Schubert, K. A.; Smith, M. A., In situ oxidative catalysis by neurofibrillary tangles and senile plaques in Alzheimer's disease: a central role for bound transition metals. *J Neurochem* **2000,** *74* (1), 270-9.

40.   Su, X.-Y.; Wu, W.-H.; Huang, Z.-P.; Hu, J.; Lei, P.; Yu, C.-H.; Zhao, Y.-F.; Li, Y.-M., Hydrogen peroxide can be generated by tau in the presence of Cu(II). *Biochemical and biophysical research communications* **2007,** *358* (2), 661-665.

41.   Walker, S.; Ullman, O.; Stultz, C. M., Using intramolecular disulfide bonds in tau protein to deduce structural features of aggregation-resistant conformations. *J Biol Chem* **2012,** *287* (12), 9591-600.

42.   Furukawa, Y.; Kaneko, K.; Nukina, N., Tau protein assembles into isoform- and disulfide-dependent polymorphic fibrils with distinct structural properties. *J Biol Chem* **2011,** *286* (31), 27236-46.

43.   Pirota, V.; Dell'Acqua, S.; Monzani, E.; Nicolis, S.; Casella, L., Copper-Aβ Peptides and Oxidation of Catecholic Substrates: Reactivity and Endogenous Peptide Damage. *Chemistry – A European Journal* **2016,** *22* (47), 16964-16973.

44.   Ciregna, D.; Monzani, E.; Thiabaud, G.; Pizzocaro, S.; Casella, L., Copper-β-amyloid peptides exhibit neither monooxygenase nor superoxide dismutase activities. *Chem Commun (Camb)* **2013,** *49* (38), 4027-9.

45.   De Ricco, R.; Valensin, D.; Dell'Acqua, S.; Casella, L.; Hureau, C.; Faller, P., Copper(I/II), alpha/beta-Synuclein and Amyloid-beta: Menage a Trois? *Chembiochem* **2015,** *16* (16), 2319-28.

46.   Dell'Acqua, S.; Pirota, V.; Anzani, C.; Rocco, M. M.; Nicolis, S.; Valensin, D.; Monzani, E.; Casella, L., Reactivity of copper-[small alpha]-synuclein peptide complexes relevant to Parkinson's disease. *Metallomics* **2015,** *7* (7), 1091-1102.

47.   Dell'Acqua, S.; Pirota, V.; Monzani, E.; Camponeschi, F.; De Ricco, R.; Valensin, D.; Casella, L., Copper(I) Forms a Redox-Stable 1:2 Complex with α-Synuclein N-Terminal Peptide in a Membrane-Like Environment. *Inorganic Chemistry* **2016,** *55* (12), 6100-6106.

48.   Dell'Acqua, S.; Bacchella, C.; Monzani, E.; Nicolis, S.; Di Natale, G.; Rizzarelli, E.; Casella, L., Prion Peptides Are Extremely Sensitive to Copper Induced Oxidative Stress. *Inorg Chem* **2017,** *56* (18), 11317-11325.

49.   Billo, E. J., Copper(II) chromosomes and the rule of average environment. *Inorganic and Nuclear Chemistry Letters* **1974,** *10* (8), 613-617.

50.   Prenesti, E.; Daniele, P. G.; Prencipe, M.; Ostacoli, G., Spectrum-structure correlation for visible absorption spectra of copper(II) complexes in aqueous solution. *Polyhedron* **1999,** *18* (25), 3233-3241.

51.   Sigel, H.; Martin, R. B., Coordinating Properties of the Amide Bond. Stability and Structure of Metal Ion Complexes of Peptides and Related Ligands. *Chemical Reviews* **1982,** *82* (4), 385-426.

52.   Peisach, J.; Blumberg, W. E., Structural implications derived from the analysis of electron paramagnetic resonance spectra of natural and artificial copper proteins. *Arch Biochem Biophys* **1974,** *165* (2), 691-708.

53.   Gralka, E.; Valensin, D.; Porciatti, E.; Gajda, C.; Gaggelli, E.; Valensin, G.; Kamysz, W.; Nadolny, R.; Guerrini, R.; Bacco, D.; Remelli, M.; Kozlowski, H., CuII binding sites located at His-96 and His-111 of the human prion protein: thermodynamic and spectroscopic studies on model peptides. *Dalton Trans* **2008,** (38), 5207-19.

54.   Remelli, M.; Valensin, D.; Toso, L.; Gralka, E.; Guerrini, R.; Marzola, E.; Kozlowski, H., Thermodynamic and spectroscopic investigation on the role of Met residues in Cu(II) binding to the non-octarepeat site of the human prion protein. *Metallomics* **2012,** *4* (8), 794-806.

55.   Santagostini, L.; Gullotti, M.; Pagliarin, R.; Bianchi, E.; Casella, L.; Monzani, E., Functional mimics of copper enzymes. Synthesis and stereochemical properties of the copper(II) complexes of a trinucleating ligand derived from L-histidine. *Tetrahedron Asymmetry* **1999,** *10* (2), 281-295.

56.   Perrone, M. L.; Salvadeo, E.; Lo Presti, E.; Pasotti, L.; Monzani, E.; Santagostini, L.; Casella, L., A dinuclear biomimetic Cu complex derived from l-histidine: synthesis and stereoselective oxidations. *Dalton Trans* **2017,** *46* (12), 4018-4029.

57.   Presti, E. L.; Perrone, M. L.; Santagostini, L.; Casella, L.; Monzani, E., A Stereoselective Tyrosinase Model Compound Derived from an m-Xylyl-l-histidine Ligand. *Inorg Chem* **2019,** *58* (11), 7335-7344.

58.   Alies, B.; Renaglia, E.; Rozga, M.; Bal, W.; Faller, P.; Hureau, C., Cu(II) affinity for the Alzheimer's peptide: tyrosine fluorescence studies revisited. *Anal Chem* **2013,** *85* (3), 1501-8.

59.   Alies, B.; Badei, B.; Faller, P.; Hureau, C., Reevaluation of copper(I) affinity for amyloid-beta peptides by competition with ferrozine--an unusual copper(I) indicator. *Chemistry* **2012,** *18* (4), 1161-7.

60.   Haas, K. L.; Putterman, A. B.; White, D. R.; Thiele, D. J.; Franz, K. J., Model peptides provide new insights into the role of histidine residues as potential ligands in human cellular copper acquisition via Ctr1. *J Am Chem Soc* **2011,** *133* (12), 4427-37.

61.   Himes, R. A.; Park, G. Y.; Siluvai, G. S.; Blackburn, N. J.; Karlin, K. D., Structural studies of copper(I) complexes of amyloid-beta peptide fragments: formation of two-coordinate bis(histidine) complexes. *Angew Chem Int Ed Engl* **2008,** *47* (47), 9084-7.

62.	Conklin, S. E.; Bridgman, E. C.; Su, Q.; Riggs-Gelasco, P.; Haas, K. L.; Franz, K. J., Specific Histidine Residues Confer Histatin Peptides with Copper-Dependent Activity against Candida albicans. *Biochemistry* **2017**, *56* (32), 4244-4255.

63.	Gaggelli, E.; D'Amelio, N.; Valensin, D.; Valensin, G., 1H NMR studies of copper binding by histidine-containing peptides. *Magnetic Resonance in Chemistry* **2003**, *41* (10), 877-883.

64.	Gaggelli, E.; Kozlowski, H.; Valensin, D.; Valensin, G., NMR studies on Cu(II)-peptide complexes: Exchange kinetics and determination of structures in solution. *Molecular BioSystems* **2005**, *1* (1), 79-84.

65.	Hautier, A.; Carvalho, T.; Valensin, D.; Simaan, A. J.; Faure, B.; Mateus, P.; Delgado, R.; Iranzo, O., The role of methylation in the copper(ii) coordination properties of a His-containing decapeptide. *Dalton Trans* **2019**, *48* (5), 1859-1870.

66.	De Gregorio, G.; Biasotto, F.; Hecel, A.; Luczkowski, M.; Kozlowski, H.; Valensin, D., Structural analysis of copper(I) interaction with amyloid beta peptide. *J Inorg Biochem* **2019**, *195*, 31-38.

67.	Valensin, D.; Padula, E. M.; Hecel, A.; Luczkowski, M.; Kozlowski, H., Specific binding modes of Cu(I) and Ag(I) with neurotoxic domain of the human prion protein. *J Inorg Biochem* **2016**, *155*, 26-35.

68.	Atrian-Blasco, E.; Gonzalez, P.; Santoro, A.; Alies, B.; Faller, P.; Hureau, C., Cu and Zn coordination to amyloid peptides: From fascinating chemistry to debated pathological relevance. *Coord Chem Rev* **2018**, *375*, 38-55.

69.	Shearer, J.; Szalai, V. A., The amyloid-beta peptide of Alzheimer's disease binds Cu(I) in a linear bis-his coordination environment: insight into a possible neuroprotective mechanism for the amyloid-beta peptide. *J Am Chem Soc* **2008**, *130* (52), 17826-35.

70.	Monzani, E.; Nicolis, S.; Dell'Acqua, S.; Capucciati, A.; Bacchella, C.; Zucca, F. A.; Mosharov, E. V.; Sulzer, D.; Zecca, L.; Casella, L., Dopamine, Oxidative Stress and Protein-Quinone Modifications in Parkinson's and Other Neurodegenerative Diseases. *Angew Chem Int Ed Engl* **2019**, *58* (20), 6512-6527.

71.	Zecca, L.; Bellei, C.; Costi, P.; Albertini, A.; Monzani, E.; Casella, L.; Gallorini, M.; Bergamaschi, L.; Moscatelli, A.; Turro, N. J.; Eisner, M.; Crippa, P. R.; Ito, S.; Wakamatsu, K.; Bush, W. D.; Ward, W. C.; Simon, J. D.; Zucca, F. A., New melanic pigments in the human brain that accumulate in aging and block environmental toxic metals. *Proceedings of the National Academy of Sciences* **2008**, *105* (45), 17567-17572.

72.	Pham, A. N.; Waite, T. D., Cu(II)-catalyzed oxidation of dopamine in aqueous solutions: mechanism and kinetics. *J Inorg Biochem* **2014**, *137*, 74-84.

73.	Herlinger, E.; Jameson, R. F.; Linert, W., Spontaneous autoxidation of dopamine. *Journal of the Chemical Society, Perkin Transactions 2* **1995**, (2), 259-263.

74.	da Silva, G. F. Z.; Ming, L.-J., Metallo-ROS in Alzheimer's Disease: Oxidation of Neurotransmitters by CuII-β-Amyloid and Neuropathology of the Disease. *Angewandte Chemie International Edition* **2007**, *46* (18), 3337-3341.

75.	Nam, E.; Derrick, J. S.; Lee, S.; Kang, J.; Han, J.; Lee, S. J. C.; Chung, S. W.; Lim, M. H., Regulatory Activities of Dopamine and Its Derivatives toward Metal-Free and Metal-Induced Amyloid-β Aggregation, Oxidative Stress, and Inflammation in Alzheimer's Disease. *ACS Chemical Neuroscience* **2018**, *9* (11), 2655-2666.

76.	Atrián-Blasco, E.; Del Barrio, M.; Faller, P.; Hureau, C., Ascorbate Oxidation by Cu(Amyloid-β) Complexes: Determination of the Intrinsic Rate as a Function of Alterations in the Peptide Sequence Revealing Key Residues for Reactive Oxygen Species Production. *Analytical Chemistry* **2018**, *90* (9), 5909-5915.

77.	Yako, N.; Young, T. R.; Cottam Jones, J. M.; Hutton, C. A.; Wedd, A. G.; Xiao, Z., Copper binding and redox chemistry of the Aβ16 peptide and its variants: insights into determinants of copper-dependent reactivity. *Metallomics : integrated biometal science* **2017**, *9* (3), 278-291.

78.	Solomon, E. I.; Heppner, D. E.; Johnston, E. M.; Ginsbach, J. W.; Cirera, J.; Qayyum, M.; Kieber-Emmons, M. T.; Kjaergaard, C. H.; Hadt, R. G.; Tian, L., Copper Active Sites in Biology. *Chemical Reviews* **2014**, *114* (7), 3659-3853.

79.	Smith, D. G.; Cappai, R.; Barnham, K. J., The redox chemistry of the Alzheimer's disease amyloid beta peptide. *Biochim Biophys Acta* **2007**, *1768* (8), 1976-90.

80.	Chassaing, S.; Collin, F.; Dorlet, P.; Gout, J.; Hureau, C.; Faller, P., Copper and heme-mediated Abeta toxicity: redox chemistry, Abeta oxidations and anti-ROS compounds. *Curr Top Med Chem* **2012**, *12* (22), 2573-95.

81.	Butterfield, D. A.; Reed, T.; Newman, S. F.; Sultana, R., Roles of amyloid beta-peptide-associated oxidative stress and brain protein modifications in the pathogenesis of Alzheimer's disease and mild cognitive impairment. *Free Radic Biol Med* **2007**, *43* (5), 658-77.

82.	Hawkins, C. L.; Davies, M. J., Generation and propagation of radical reactions on proteins. *Biochim Biophys Acta* **2001**, *1504* (2-3), 196-219.

83.	Hureau, C.; Faller, P., Abeta-mediated ROS production by Cu ions: structural insights, mechanisms and relevance to Alzheimer's disease. *Biochimie* **2009**, *91* (10), 1212-7.

84.	Requena, J. R.; Chao, C.-C.; Levine, R. L.; Stadtman, E. R., Glutamic and aminoadipic semialdehydes are the main carbonyl products of metal-catalyzed oxidation of proteins. *Proceedings of the National Academy of Sciences* **2001**, *98* (1), 69.
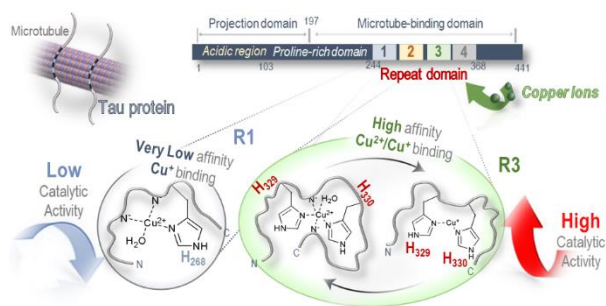
Table of Contents Artwork

Table of Contents Synopsis: This study presents a detailed and quantitative analysis of the binding of copper with R1 and R3 fragments of tau protein, which are involved in microtubule-binding domain. The presence of two consequent histidine residues in R3 portion confers a suitable coordination for copper in both oxidation states, thus enhancing the copper-mediated oxygen reactions. Conversely, the binding of copper to R1 fragment has a low effect on oxygen activation reactions.